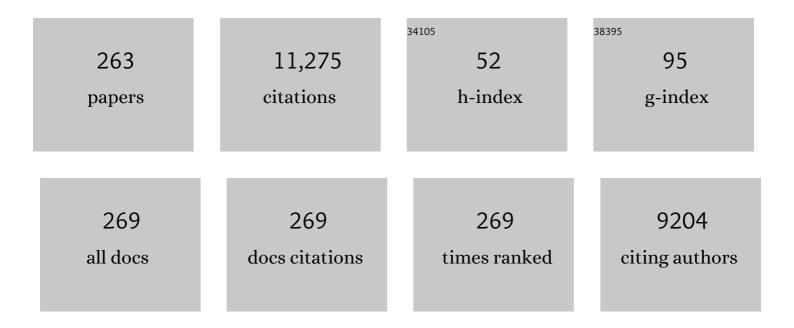
List of Publications by Year in descending order

Source: https://exaly.com/author-pdf/6503620/publications.pdf Version: 2024-02-01



 #	Article	IF	CITATIONS
1	Influence of Crystal Structure, Encapsulation, and Annealing on Photochromism in Nd Oxyhydride Thin Films. Journal of Physical Chemistry C, 2022, 126, 2276-2284. Energy, metastability, and optical properties of anion-disordered <mml:math< th=""><th>3.1</th><th>8</th></mml:math<>	3.1	8
	xmlns;mml="http://www.w3'org/1998/Math/MathMI"> <mml·mrow><mml·mi>R</mml·mi><mml·msub><mml·mi< td=""><td></td><td></td></mml·mi<></mml·msub></mml·mrow>		

xmlns:mml="http://www.w3.org/1998/Math/MathML"> < mml:mrow> < mml:mi>R</mml:mi> < mml:msub> < mml:mi mathvariant="normal">O</mml:mi> < mml:mi> x</mml:mi> </mml:msub> < mml:mi mathvariant="normal">H</mml:mi> < mml:mrow> < mml:mn> 3 </mml:mn> < mml:mo> â^2 </mml:mo> < mml:mn> 2 </mml:mn> < mml:mi> x</n 2 <mml:math

#	Article	IF	CITATIONS
19	Designing Reliable Operando TEM Experiments to Study (De)lithiation Mechanism of Battery Electrodes. Journal of the Electrochemical Society, 2019, 166, A3384-A3386.	2.9	2
20	Optical hydrogen sensing beyond palladium: Hafnium and tantalum as effective sensing materials. Sensors and Actuators B: Chemical, 2019, 283, 538-548.	7.8	26
21	Effect of the addition of zirconium on the photochromic properties of yttrium oxy-hydride. Solar Energy Materials and Solar Cells, 2019, 200, 109923.	6.2	12
22	Oxyhydride Nature of Rare-Earth-Based Photochromic Thin Films. Journal of Physical Chemistry Letters, 2019, 10, 1342-1348.	4.6	45
23	Suppressing H ₂ Evolution and Promoting Selective CO ₂ Electroreduction to CO at Low Overpotentials by Alloying Au with Pd. ACS Catalysis, 2019, 9, 3527-3536.	11.2	79
24	Direct Comparison of PdAu Alloy Thin Films and Nanoparticles upon Hydrogen Exposure. ACS Applied Materials & Interfaces, 2019, 11, 15489-15497.	8.0	45
25	Metal–polymer hybrid nanomaterials for plasmonic ultrafast hydrogen detection. Nature Materials, 2019, 18, 489-495.	27.5	227
26	Electronic structure and vacancy formation in photochromic yttrium oxy-hydride thin films studied by positron annihilation. Solar Energy Materials and Solar Cells, 2018, 177, 97-105.	6.2	13
27	Elastic versus Alloying Effects in Mg-Based Hydride Films. Physical Review Letters, 2018, 121, 255503.	7.8	23
28	Hydrogen storage in Mg2FeSi alloy thin films depending on the Fe-to-Si ratio measured by conversion electron M¶ssbauer spectroscopy. Nuclear Instruments & Methods in Physics Research B, 2018, 434, 109-112.	1.4	3
29	Pathways to electrochemical solar-hydrogen technologies. Energy and Environmental Science, 2018, 11, 2768-2783.	30.8	238
30	Hafnium—an optical hydrogen sensor spanning six orders in pressure. Nature Communications, 2017, 8, 15718.	12.8	41
31	Functionalised metal–organic frameworks: a novel approach to stabilising single metal atoms. Journal of Materials Chemistry A, 2017, 5, 15559-15566.	10.3	24
32	Enhancement of Destabilization and Reactivity of Mg Hydride Embedded in Immiscible Ti Matrix by Addition of Cr: Pd-Free Destabilized Mg Hydride. Journal of Physical Chemistry C, 2017, 121, 12631-12635.	3.1	11
33	Photochromism of rare-earth metal-oxy-hydrides. Applied Physics Letters, 2017, 111, .	3.3	55
34	Metal-hydrogen systems with an exceptionally large and tunable thermodynamic destabilization. Nature Communications, 2017, 8, 1846.	12.8	47
35	The Impact of Post-Synthetic Linker Functionalization of MOFs on Methane Storage: The Role of Defects. Frontiers in Energy Research, 2016, 4, .	2.3	16
36	Promotion of Hydrogen Desorption from Palladium Surfaces by Fluoropolymer Coating. ChemCatChem, 2016, 8, 1646-1650.	3.7	19

#	Article	IF	CITATIONS
37	Deposition of conductive TiN shells on SiO2 nanoparticles with a fluidized bed ALD reactor. Journal of Nanoparticle Research, 2016, 18, 1.	1.9	2
38	Nanostructured materials for solid-state hydrogen storage: A review of the achievement of COST Action MP1103. International Journal of Hydrogen Energy, 2016, 41, 14404-14428.	7.1	94
39	Impact of Nanostructuring on the Phase Behavior of Insertion Materials: The Hydrogenation Kinetics of a Magnesium Thin Film. Journal of Physical Chemistry C, 2016, 120, 10185-10191.	3.1	23
40	Photoelectrochemical water splitting with porous α-Fe2O3 thin films prepared from Fe/Fe-oxide nanoparticles. Applied Catalysis A: General, 2016, 523, 130-138.	4.3	35
41	Review of magnesium hydride-based materials: development and optimisation. Applied Physics A: Materials Science and Processing, 2016, 122, 1.	2.3	274
42	Amorphous Metal-Hydrides for Optical Hydrogen Sensing: The Effect of Adding Glassy Ni–Zr to Mg–Ni–H. ACS Sensors, 2016, 1, 222-226.	7.8	17
43	Interface and strain effects on the H-sorption thermodynamics of size-selected Mg nanodots. International Journal of Hydrogen Energy, 2016, 41, 9841-9851.	7.1	12
44	Searching for Ti-clusters in Mg0.7Ti0.3 thin film. Acta Crystallographica Section A: Foundations and Advances, 2016, 72, s159-s159.	0.1	0
45	Photocorrosion Mechanism of TiO ₂ -Coated Photoanodes. International Journal of Photoenergy, 2015, 2015, 1-8.	2.5	18
46	Gradient dopant profiling and spectral utilization of monolithic thin-film silicon photoelectrochemical tandem devices for solar water splitting. Journal of Materials Chemistry A, 2015, 3, 4155-4162.	10.3	35
47	The hydrogen permeability of Pd–Cu based thin film membranes in relation to their structure: A combinatorial approach. International Journal of Hydrogen Energy, 2015, 40, 3932-3943.	7.1	16
48	Solar Water Splitting Combining a BiVO ₄ Light Absorber with a Ru-Based Molecular Cocatalyst. Journal of Physical Chemistry C, 2015, 119, 7275-7281.	3.1	75
49	Destabilization of Mg Hydride by Self-Organized Nanoclusters in the Immiscible Mg–Ti System. Journal of Physical Chemistry C, 2015, 119, 12157-12164.	3.1	30
50	Optical hydrogen sensing with nanoparticulate Pd–Au films produced by spark ablation. Sensors and Actuators B: Chemical, 2015, 221, 290-296.	7.8	26
51	Extracting large photovoltages from a-SiC photocathodes with an amorphous TiO ₂ front surface field layer for solar hydrogen evolution. Energy and Environmental Science, 2015, 8, 1585-1593.	30.8	74
52	Oxynitrogenography: Controlled Synthesis of Single-Phase Tantalum Oxynitride Photoabsorbers. Chemistry of Materials, 2015, 27, 7091-7099.	6.7	59
53	Contaminant-resistant MOF–Pd composite for H ₂ separation. RSC Advances, 2015, 5, 89323-89326.	3.6	1
54	A simple route for preparation of textured WO3 thin films from colloidal W nanoparticles and their photoelectrochemical water splitting properties. Applied Catalysis B: Environmental, 2015, 166-167, 406-412.	20.2	27

#	Article	IF	CITATIONS
55	Seeing Hydrogen in Colors: Lowâ€Cost and Highly Sensitive Eye Readable Hydrogen Detectors. Advanced Functional Materials, 2014, 24, 2374-2382.	14.9	78
56	Unraveling the Carrier Dynamics of BiVO ₄ : A Femtosecond to Microsecond Transient Absorption Study. Journal of Physical Chemistry C, 2014, 118, 27793-27800.	3.1	142
57	Eye readable metal hydride based hydrogen tape sensor for health applications. Proceedings of SPIE, 2014, , .	0.8	3
58	Optical modeling of an efficient water splitting device based on bismuth vanadate photoanode and micromorph silicon solar cells. , 2014, , .		3
59	Fiber optic hydrogen sensor for a continuously monitoring of the partial hydrogen pressure in the natural gas grid. Sensors and Actuators B: Chemical, 2014, 199, 127-132.	7.8	21
60	Probing hydrogen spillover in Pd@MIL-101(Cr) with a focus on hydrogen chemisorption. Physical Chemistry Chemical Physics, 2014, 16, 5803.	2.8	33
61	A novel approach for the preparation of textured CuO thin films from electrodeposited CuCl and CuBr. Journal of Electroanalytical Chemistry, 2014, 717-718, 243-249.	3.8	37
62	Optical fiber sensor for the continuous monitoring of hydrogen in oil. Sensors and Actuators B: Chemical, 2014, 190, 982-989.	7.8	62
63	Optimization of amorphous silicon double junction solar cells for an efficient photoelectrochemical water splitting device based on a bismuth vanadate photoanode. Physical Chemistry Chemical Physics, 2014, 16, 4220-4229.	2.8	40
64	Interplay of Linker Functionalization and Hydrogen Adsorption in the Metal–Organic Framework MIL-101. Journal of Physical Chemistry C, 2014, 118, 19572-19579.	3.1	22
65	Plasmonic enhancement of the optical absorption and catalytic efficiency of BiVO4 photoanodes decorated with Ag@SiO2 core–shell nanoparticles. Physical Chemistry Chemical Physics, 2014, 16, 15272-15277.	2.8	61
66	A Bismuth Vanadate–Cuprous Oxide Tandem Cell for Overall Solar Water Splitting. Journal of Physical Chemistry C, 2014, 118, 16959-16966.	3.1	226
67	Highly sensitive and selective visual hydrogen detectors based on YxMg1â^'x thin films. Sensors and Actuators B: Chemical, 2014, 203, 745-751.	7.8	17
68	Solid-State NMR Studies of the Photochromic Effects of Thin Films of Oxygen-Containing Yttrium Hydride. Journal of Physical Chemistry C, 2014, 118, 22935-22942.	3.1	34
69	Efficient Waterâ€Splitting Device Based on a Bismuth Vanadate Photoanode and Thinâ€Film Silicon Solar Cells. ChemSusChem, 2014, 7, 2832-2838.	6.8	149
70	Hydride destabilization in core–shell nanoparticles. International Journal of Hydrogen Energy, 2014, 39, 2115-2123.	7.1	33
71	The effect of microstructure on the hydrogenation of Mg/Fe thin film multilayers. International Journal of Hydrogen Energy, 2014, 39, 17092-17103.	7.1	17
72	Polymerâ€Induced Surface Modifications of Pdâ€based Thin Films Leading to Improved Kinetics in Hydrogen Sensing and Energy Storage Applications. Angewandte Chemie - International Edition, 2014, 53, 12081-12085.	13.8	53

#	Article	lF	CITATIONS
73	The Origin of Slow Carrier Transport in BiVO ₄ Thin Film Photoanodes: A Time-Resolved Microwave Conductivity Study. Journal of Physical Chemistry Letters, 2013, 4, 2752-2757.	4.6	478
74	Nanostructured Pd–Au based fiber optic sensors for probing hydrogen concentrations in gas mixtures. International Journal of Hydrogen Energy, 2013, 38, 4201-4212.	7.1	80
75	Efficient solar water splitting by enhanced charge separation in a bismuth vanadate-silicon tandem photoelectrode. Nature Communications, 2013, 4, 2195.	12.8	1,137
76	X-ray photoelectron spectroscopy investigation of magnetron sputtered Mg–Ti–H thin films. International Journal of Hydrogen Energy, 2013, 38, 10704-10715.	7.1	21
77	Ni and p-Cu2O Nanocubes with a Small Size Distribution by Templated Electrodeposition and Their Characterization by Photocurrent Measurement. ACS Applied Materials & Interfaces, 2013, 5, 10938-10945.	8.0	9
78	Post-synthetic cation exchange in the robust metal–organic framework MIL-101(Cr). CrystEngComm, 2013, 15, 10175.	2.6	44
79	Metal–organic framework thin films for protective coating of Pd-based optical hydrogen sensors. Journal of Materials Chemistry C, 2013, 1, 8146.	5.5	48
80	MOF@MOF core–shell vs. Janus particles and the effect of strain: potential for guest sorption, separation and sequestration. CrystEngComm, 2013, 15, 6003.	2.6	40
81	Study of a fiber optic sensor for hydrogen leak detection. , 2013, , .		1
82	Hysteresis and the role of nucleation and growth in the hydrogenation of Mg nanolayers. Physical Chemistry Chemical Physics, 2013, 15, 2782.	2.8	44
83	The clamping effect in the complex hydride Mg2NiH4 thin films. Journal of Materials Chemistry A, 2013, 1, 10972.	10.3	8
84	Nucleation and growth mechanisms of nano magnesium hydride from the hydrogen sorption kinetics. Physical Chemistry Chemical Physics, 2013, 15, 11501.	2.8	59
85	Photoelectrochemical Properties of Cadmium Chalcogenide-Sensitized Textured Porous Zinc Oxide Plate Electrodes. ACS Applied Materials & amp; Interfaces, 2013, 5, 1113-1121.	8.0	57
86	Combinatorial method for direct measurements of the intrinsic hydrogen permeability of separation membrane materials. Journal of Membrane Science, 2013, 444, 70-76.	8.2	5
87	A reliable, sensitive and fast optical fiber hydrogen sensor based on surface plasmon resonance. Optics Express, 2013, 21, 382.	3.4	124
88	Metal hydrides for smart window and sensor applications. MRS Bulletin, 2013, 38, 495-503.	3.5	48
89	Innovative fiber optic sensor for hydrogen detection. , 2012, , .		1
90	Optical hydrogen sensors based on metal-hydrides. Proceedings of SPIE, 2012, , .	0.8	10

#	Article	IF	CITATIONS
91	Magnesium Nanoparticles for Hydrogen Storage: Structure, Kinetics and Thermodynamics. IOP Conference Series: Materials Science and Engineering, 2012, 38, 012001.	0.6	7
92	Effect of the structure transformation on the (de-)hydrogenation hysteresis of La1â^'zYzHx films as studied by hydrogenography. Journal of Materials Chemistry, 2012, 22, 24453.	6.7	4
93	Thermal Stability of MgyTi1-y Thin Films Investigated by Positron Annihilation Spectroscopy. Physics Procedia, 2012, 35, 16-21.	1.2	8
94	Thermodynamic Properties, Hysteresis Behavior and Stress-Strain Analysis of MgH2 Thin Films, Studied over a Wide Temperature Range. Crystals, 2012, 2, 710-729.	2.2	20
95	Combined XPS and first principle study of metastable Mg–Ti thin films. Surface and Interface Analysis, 2012, 44, 986-988.	1.8	6
96	EXAFS investigation of the destabilization of the Mg–Ni–Ti (H) system. International Journal of Hydrogen Energy, 2012, 37, 4161-4169.	7.1	13
97	Thin film based sensors for a continuous monitoring of hydrogen concentrations. Sensors and Actuators B: Chemical, 2012, 165, 88-96.	7.8	23
98	In-situ TEM on (de)hydrogenation of Pd at 0.5–4.5 bar hydrogen pressure and 20–400°C. Ultramicroscopy, 2012, 112, 47-52.	1.9	77
99	Siting and Mobility of Deuterium Absorbed in Cosputtered Mg0.65Ti0.35. A MAS 2H NMR Study. Journal of Physical Chemistry C, 2011, 115, 288-297.	3.1	15
100	Thin film metal hydrides for hydrogen storage applications. Journal of Materials Chemistry, 2011, 21, 4021-4026.	6.7	44
101	Titanium nitride: A new Ohmic contact material for n-type CdS. Journal of Applied Physics, 2011, 110, .	2.5	28
102	Fiber optic Surface Plasmon Resonance sensor based on wavelength modulation for hydrogen sensing. Optics Express, 2011, 19, A1175.	3.4	93
103	Layer-resolved study of the Mg to MgH2 transformation in Mg–Ti films with short-range chemical order. Journal of Alloys and Compounds, 2011, 509, S567-S571.	5.5	12
104	A new thin film photochromic material: Oxygen-containing yttrium hydride. Solar Energy Materials and Solar Cells, 2011, 95, 3596-3599.	6.2	90
105	Interface Energy Controlled Thermodynamics of Nanoscale Metal Hydrides. Advanced Energy Materials, 2011, 1, 754-758.	19.5	68
106	High throughput screening of Pd-alloys for H2 separation membranes studied by hydrogenography and CVM. International Journal of Hydrogen Energy, 2011, 36, 1074-1082.	7.1	17
107	Thermodynamics, stress release and hysteresis behavior inÂhighly adhesive Pd–H films. International Journal of Hydrogen Energy, 2011, 36, 4056-4067.	7.1	53
108	Optical response of the sodium alanate system: <mml:math xmlns:mml="http://www.w3.org/1998/Math/MathML" display="inline"><mml:mrow><mml:msub><mml:mi mathyariant="italia">CW//mml:mi><mml:mrow>O//mml:mn></mml:mrow></mml:mi </mml:msub></mml:mrow></mml:math 	3.12 ml	mathy DCE

mathvariant="italic">GW</mml:mi><mml:mrow><mml:mn>Ó</mml:mn></mml:mrow></mml:msub></mml:mrow></mml:mrow></mml:mrow></mml:mrow></mml:mrow></mml:mrow></mml:mrow></mml:mrow></mml:mrow></mml:mrow></mml:mrow></mml:mrow></mml:mrow></mml:mrow></mml:mrow></mml:mrow></mml:mrow></mml:mrow></mml:mrow></mml:mrow></mml:mrow></mml:mrow></mml:mrow></mml:mrow></mml:mrow></mml:mrow></mml:mrow></mml:mrow></mml:mrow></mml:mrow></mml:mrow></mml:mrow></mml:mrow></mml:mrow></mml:mrow></mml:mrow></mml:mrow></mml:mrow></mml:mrow></mml:mrow></mml:mrow></mml:mrow></mml:mrow></mml:mrow></mml:mrow></mml:mrow></mml:mrow></mml:mrow></mml:mrow></mml:mrow></mml:mrow></mml:mrow></mml:mrow></mml:mrow></mml:mrow></mml:mrow></mml:mrow></mml:mrow></mml:mrow></mml:mrow></mml:mrow></mml:mrow></mml:mrow></mml:mrow></mml:mrow></mml:mrow></mml:mrow></mml:mrow></mml:mrow></mml:mrow></mml:mrow></mml:mrow></mml:mrow></mml:mrow></mml:mrow></mml:mrow></mml:mrow></mml:mrow></mml:mrow></mml:mrow></mml:mrow></mml:mrow></mml:mrow></mml:mrow></mml:mrow></mml:mrow></mml:mrow></mml:mrow></mml:mrow></mml:mrow></mml:mrow></mml:mrow></mml:mrow></mml:mrow></mml:mrow></mml:mrow></mml:mrow></mml:mrow></mml:mrow></mml:mrow></mml:mrow></mml:mrow></mml:mrow></mml:mrow></mml:mrow></mml:mrow></mml:mrow></mml:mrow></mml:mrow></mml:mrow></mml:mrow></mml:mrow></mml:mrow></mml:mrow></mml:mrow></mml:mrow></mml:mrow></mml:mrow></mml:mrow></mml:mrow></mml:mrow></mml:mrow></mml:mrow></mml:mrow></mml:mrow></mml:mrow></mml:mrow></mml:mrow></mml:mrow></mml:mrow></mml:mrow></mml:mrow></mml:mrow></mml:mrow></mml:mrow></mml:mrow></mml:mrow></mml:mrow></mml:mrow></mml:mrow></mml:mrow></mml:mrow></mml:mrow></mml:mrow></mml:mrow></mml:mrow></mml:mrow></mml:mrow></mml:mrow></mml:mrow></mml:mrow></mml:mrow></mml:mrow></mml:mrow></mml:mrow></mml:mrow></mml:mrow></mml:mrow></mml:mrow></mml:mrow></mml:mrow></mml:mrow></mml:mrow></mml:mrow></mml:mrow></mml:mrow></mml:mrow></mml:mrow></mml:mrow></mml:mrow></mml:mrow></mml:mrow></mml:mrow></mml:mrow></mml:mrow></mml:mrow></mml:mrow></mml:mrow></mml:

#	Article	IF	CITATIONS
109	Optimization of Pd surface plasmon resonance sensors for hydrogen detection. , 2011, , .		1
110	Wavelength response of a surface plasmon resonance palladium-coated optical fiber sensor for hydrogen detection. Optical Engineering, 2011, 50, 014403.	1.0	17
111	Hydrogenography of Mg Ni1â^'H gradient thin films: Interplay between the thermodynamics and kinetics of hydrogenation. Acta Materialia, 2010, 58, 658-668.	7.9	29
112	Effect of H-induced microstructural changes on pressure-optical transmission isotherms for Mg–V thin films. International Journal of Hydrogen Energy, 2010, 35, 6959-6970.	7.1	9
113	An optical hydrogen sensor based on a Pd-capped Mg thin film wedge. International Journal of Hydrogen Energy, 2010, 35, 12574-12578.	7.1	32
114	Xâ€ray photoelectron spectroscopy study of MgH ₂ thin films grown by reactive sputtering. Surface and Interface Analysis, 2010, 42, 1140-1143.	1.8	2
115	A distributed optical fiber sensor for hydrogen detection based on Pd, and Mg alloys. Proceedings of SPIE, 2010, , .	0.8	0
116	Thermal stability of gas phase magnesium nanoparticles. Journal of Applied Physics, 2010, 107, 053504.	2.5	34
117	Mg/Ti multilayers: Structural and hydrogen absorption properties. Physical Review B, 2010, 81, .	3.2	52
118	Divacancies and the hydrogenation of Mg-Ti films with short range chemical order. Applied Physics Letters, 2010, 96, .	3.3	21
119	In-Situ Deposition of Alkali and Alkaline Earth Hydride Thin Films To Investigate the Formation of Reactive Hydride Composites. Journal of Physical Chemistry C, 2010, 114, 13895-13901.	3.1	11
120	Destabilization of the Mg-H System through Elastic Constraints. Physical Review Letters, 2009, 102, 226102.	7.8	157
121	Positron depth profiling of the structural and electronic structure transformations of hydrogenated Mg-based thin films. Journal of Applied Physics, 2009, 105, .	2.5	30
122	Quasifree Mg–H thin films. Applied Physics Letters, 2009, 95, .	3.3	57
123	Effect of the substrate on the thermodynamic properties of PdHx films studied by hydrogenography. Scripta Materialia, 2009, 60, 348-351.	5.2	50
124	Nanoscale composition modulations in MgyTi1â^'yHx thin film alloys for hydrogen storage. International Journal of Hydrogen Energy, 2009, 34, 1450-1457.	7.1	52
125	Structural and optical properties of MgyNi1–yHx gradient thin films in relation to the as-deposited metallic state. International Journal of Hydrogen Energy, 2009, 34, 8951-8957.	7.1	24
126	Hydrogenography of PdHx thin films: Influence of H-induced stress relaxation processes. Acta Materialia, 2009, 57, 1209-1219.	7.9	54

#	Article	IF	CITATIONS
127	Lightweight sodium alanate thin films grown by reactive sputtering. Applied Physics Letters, 2009, 95, 121904.	3.3	13
128	Study of the hydride forming process of in-situ grown MgH2 thin films by activated reactive evaporation. Thin Solid Films, 2008, 516, 4351-4359.	1.8	40
129	Optimization of Mg-based fiber optic hydrogen detectors by alloying the catalyst. International Journal of Hydrogen Energy, 2008, 33, 1084-1089.	7.1	64
130	Mg–Ti–H thin films as switchable solar absorbers. International Journal of Hydrogen Energy, 2008, 33, 3188-3192.	7.1	41
131	In situ electrochemical XRD study of (de)hydrogenation of MgyTi100â^'y thin films. Journal of Materials Chemistry, 2008, 18, 3680.	6.7	42
132	Highly destabilized Mg-Ti-Ni-H system investigated by density functional theory and hydrogenography. Physical Review B, 2008, 77, . Chemical short-range order and lattice deformations in smml:math	3.2	39
133	xmlns:mml="http://www.w3.org/1998/Math/MathML" display="inline"> <mml:mrow><mml:msub><mml:mi mathvariant="normal">Mg<mml:mi>y</mml:mi></mml:mi </mml:msub><mml:msub><mml:mi mathvariant="normal">Ti<mml:mrow><mml:mn>1</mml:mn><mml:mo>â^²</mml:mo><mml:mi>ymathvariant="normal">H</mml:mi><mml:mi>x</mml:mi></mml:mrow></mml:mi </mml:msub></mml:mrow> thin	۱mi:thi> <td>nmål?mrow><</td>	nmål?mrow><
134	films probed by hydrogenography. Physical Review B, 2008, 77, . Electrohydrogenation of MgH2-thin films. Applied Physics Letters, 2007, 90, 071912.	3.3	25
135	Structural, optical, and electrical properties ofMgyTi1â^'yHxthin films. Physical Review B, 2007, 75, .	3.2	116
136	Critical composition dependence of the hydrogenation of Mg2±δNi thin films. Journal of Alloys and Compounds, 2007, 428, 34-39.	5.5	8
137	The dielectric function of Mgy NiHx thin films (). Journal of Alloys and Compounds, 2007, 430, 13-18.	5.5	20
138	Influence of the Chemical Potential on the Hydrogen Sorption Kinetics of Mg2Ni/TM/Pd (TM =) Tj ETQq0 0 0 rgB ⁻	[/Qverlocl	۶ 10 Tf 50 30
139	An optical method to determine the thermodynamics of hydrogen absorption and desorption in metals. Applied Physics Letters, 2007, 91, 231916.	3.3	73
140	Hydrogenography: An Optical Combinatorial Method To Find New Lightâ€Weight Hydrogenâ€Storage Materials. Advanced Materials, 2007, 19, 2813-2817.	21.0	186
141	Opto-mechanical characterization of hydrogen storage properties of Mg–Ni thin film composition spreads. Applied Surface Science, 2007, 254, 682-686.	6.1	34
142	Fiber optic hydrogen detectors containing Mg-based metal hydrides. Sensors and Actuators B: Chemical, 2007, 123, 538-545.	7.8	104
143	Combinatorial thin film methods for the search of new lightweight metal hydrides. Scripta Materialia, 2007, 56, 853-858.	5.2	56
144	Stabilized switchable "black state―in Mg2NiH4â^•Tiâ^•Pd thin films for optical hydrogen sensing. Applied Physics Letters, 2006, 89, 021913.	3.3	32

#	Article	IF	CITATIONS
145	The growth-induced microstructural origin of the optical black state of Mg2NiHx thin films. Journal of Alloys and Compounds, 2006, 416, 2-10.	5.5	21
146	High-throughput concept for tailoring switchable mirrors. Applied Surface Science, 2006, 253, 1417-1423.	6.1	29
147	Hydrogen absorption kinetics and optical properties of Pd-doped Mg thin films. Journal of Applied Physics, 2006, 100, 023515.	2.5	39
148	Structural and optical properties of MgxAl1-xHy gradient thin films: a combinatorial approach. Applied Physics A: Materials Science and Processing, 2006, 84, 77-85.	2.3	34
149	Catalytic activity of noble metals promoting hydrogen uptake. Journal of Catalysis, 2006, 239, 263-271.	6.2	53
150	Effect of the Deposition Technique on the Metallurgy and Hydrogen Storage Characteristics of Metastable Mg[sub y]Ti[sub (1â^'y)] Thin Films. Electrochemical and Solid-State Letters, 2006, 9, A520.	2.2	35
151	Mg–Ti–H thin films for smart solar collectors. Applied Physics Letters, 2006, 88, 241910.	3.3	86
152	Optical, structural, and electrical properties of Mg2NiH4 thin films in situ grown by activated reactive evaporation. Journal of Applied Physics, 2006, 100, 063518.	2.5	29
153	The role of niobium oxide as a surface catalyst for hydrogen absorption. Journal of Catalysis, 2005, 235, 353-358.	6.2	41
154	Double layer formation in Mg–TM switchable mirrors (TM: Ni, Co, Fe). Journal of Alloys and Compounds, 2005, 404-406, 490-493.	5.5	18
155	Electrical and optical properties of epitaxial YHx switchable mirrors. Journal of Alloys and Compounds, 2005, 397, 9-16.	5.5	13
156	Thermochromic metal-hydride bilayer devices. Journal of Alloys and Compounds, 2005, 404-406, 465-468.	5.5	6
157	Combinatorial method for the development of a catalyst promoting hydrogen uptake. Journal of Alloys and Compounds, 2005, 404-406, 699-705.	5.5	31
158	Ti-catalyzed Mg(AlH4)2: A reversible hydrogen storage material. Journal of Alloys and Compounds, 2005, 404-406, 775-778.	5.5	36
159	Microstructural origin of the optical black state in Mg2NiHx thin films. Journal of Alloys and Compounds, 2005, 404-406, 481-484.	5.5	7
160	Self-Organized Layered Hydrogenation in BlackMg2NiHxSwitchable Mirrors. Physical Review Letters, 2004, 93, 197404.	7.8	69
161	Mg–Ni–H films as selective coatings: Tunable reflectance by layered hydrogenation. Applied Physics Letters, 2004, 84, 3651-3653.	3.3	42
162	Effect of the strong metal-support interaction on hydrogen sorption kinetics of Pd-capped switchable mirrors. Physical Review B, 2004, 70, .	3.2	39

#	Article	IF	CITATIONS
163	Structural and optical properties ofMg2NiHxswitchable mirrors upon hydrogen loading. Physical Review B, 2004, 70, .	3.2	79
164	Hydrogen sorption mechanism of oxidized nickel clusters. Applied Physics Letters, 2004, 85, 4884-4886.	3.3	25
165	In situ preparation of YH2 thin films by PLD for switchable devices. Journal of Alloys and Compounds, 2003, 356-357, 526-529.	5.5	12
166	The properties of pulsed laser deposited YH2 films for switchable devices. Journal of Alloys and Compounds, 2003, 356-357, 536-540.	5.5	5
167	Infinite-layer copper-oxide laser-ablated thin films: substrate, buffer-layer, and processing effects. IEEE Transactions on Applied Superconductivity, 2003, 13, 2684-2686.	1.7	5
168	Unexpected fourfold symmetry in the resistivity of patterned superconductors. Physical Review B, 2003, 67, .	3.2	46
169	Mechanism of the structural phase transformations in epitaxial YHx switchable mirrors. Journal of Applied Physics, 2002, 91, 1901-1909.	2.5	20
170	Local switching in epitaxialYHxswitchable mirrors. Physical Review B, 2002, 65, .	3.2	13
171	Strong pinning linear defects formed at the coherent growth transition of pulsed-laser-depositedYBa2Cu3O7â^îfilms. Physical Review B, 2002, 65, .	3.2	41
172	Vortex pinning by natural defects in thin films of YBa2Cu3O7â^δ. Superconductor Science and Technology, 2002, 15, 395-404.	3.5	55
173	Temperature dependence of the surface morphology of sputtered YBa2Cu3O7films. Superconductor Science and Technology, 2002, 15, 296-301.	3.5	1
174	In situ monitoring of optical and structural switching in epitaxial YHx switchable mirrors. Journal of Alloys and Compounds, 2002, 330-332, 342-347.	5.5	5
175	Magnetic force microscopy of vortex pinning at grain boundaries in superconducting thin films. Physica C: Superconductivity and Its Applications, 2002, 369, 165-170.	1.2	12
176	Growth and hydrogenation of epitaxial yttrium switchable mirrors on CaF2. Thin Solid Films, 2002, 402, 131-142.	1.8	10
177	Vortex pinning by natural linear defects in thin films ofYBa2Cu3O7â^î. Physical Review B, 2001, 64, .	3.2	119
178	Effect of the two (100) SrTiO3 substrate terminations on the nucleation and growth of YBa2Cu3O7â^'δ thin films. Physica C: Superconductivity and Its Applications, 2001, 351, 183-199.	1.2	33
179	Two-component model to describe the growth of physical-vapour-deposited YBa2Cu3O7 films. Physica C: Superconductivity and Its Applications, 2001, 356, 161-170.	1.2	4
180	Magneto-optical investigation of flux penetration in a superconducting ring. Physical Review B, 2001, 64, .	3.2	18

#	Article	IF	CITATIONS
181	NATURE OF SHARP TEMPERATURE DEPENDENCY OF NORMAL PHASE FLICKER NOISE OF EPITAXIAL YBA2CU3O7-X FILMS. , 2001, , .		2
182	Pattern formation due to non-linear vortex diffusion. Physica C: Superconductivity and Its Applications, 2000, 341-348, 1011-1014.	1.2	2
183	Magneto-optical observation of the influence of an artificial periodic magnetic pattern on the pinning of a YBa2Cu3O7â~δ thin film. Physica C: Superconductivity and Its Applications, 2000, 341-348, 1019-1022.	1.2	1
184	Controlling the natural strong pinning sites in laser ablated YBa2Cu3O7-δ thin films. Physica C: Superconductivity and Its Applications, 2000, 341-348, 2327-2330.	1.2	6
185	Vortex Pinning Regimes in thin films of YBa2Cu3O7â^î´. Physica C: Superconductivity and Its Applications, 2000, 341-348, 1463-1464.	1.2	1
186	YBa2Cu3O7â^'δ films with self-organized natural linear defects. Physica C: Superconductivity and Its Applications, 2000, 341-348, 1985-1986.	1.2	0
187	Observation of step-flow growth in laser-ablated thin films of the T′-phase compound Pr2CuO4. Physica C: Superconductivity and Its Applications, 2000, 341-348, 2355-2356.	1.2	2
188	The noise characteristics of YBCO films with strong pinning. Technical Physics Letters, 2000, 26, 1078-1080.	0.7	2
189	Natural strong pinning sites in laser-ablatedYBa2Cu3O7â~δthin films. Physical Review B, 2000, 62, 1338-1349.	3.2	89
190	Kinetic Roughening of Penetrating Flux Fronts in High-TcThin Film Superconductors. Physical Review Letters, 1999, 83, 2054-2057.	7.8	60
191	Contrast enhancement of rare-earth switchable mirrors through microscopic shutter effect. Applied Physics Letters, 1999, 75, 2050-2052.	3.3	86
192	High-quality off-stoichiometric YBa2Cu3O7â^'δ films produced by diffusion-assisted preferential laser ablation. Journal of Applied Physics, 1999, 86, 6528-6537.	2.5	17
193	Epitaxial switchable yttrium-hydride mirrors. Applied Physics Letters, 1999, 75, 1724-1726.	3.3	69
194	Temperature and magnetic-field dependence of quantum creep in various high-Tcsuperconductors. Physical Review B, 1999, 59, 7222-7237.	3.2	17
195	Hydriding kinetics of Pd capped YHx switchable mirrors. Journal of Applied Physics, 1999, 86, 6107-6119.	2.5	108
196	Origin of high critical currents in YBa2Cu3O7â^'δ superconducting thin films. Nature, 1999, 399, 439-442.	27.8	432
197	Growth-Induced Strong Pinning Sites in Laser Ablated YBa2Cu3O7-δFilms with a Non-Random Distribution. Journal of Low Temperature Physics, 1999, 117, 663-667.	1.4	5
198	Title is missing!. Journal of Low Temperature Physics, 1999, 117, 1549-1553.	1.4	0

#	Article	IF	CITATIONS
199	Anisotropy Induced Crossover from Fractal to Non-Fractal Flux Penetration in High-Tc thin Films. , 1999, , 291-306.		0
200	Strong Pinning Mechanisms in High-Tc Superconducting Yba2Cu3O7-δThin Films. , 1999, , 331-343.		1
201	Growth mode issues in epitaxy of complex oxide thin films. Journal of Materials Science: Materials in Electronics, 1998, 9, 217-226.	2.2	25
202	Visualization of hydrogen migration in solids using switchable mirrors. Nature, 1998, 394, 656-658.	27.8	152
203	The transition from 2D-nucleation to spiral growth in pulsed laser deposited YBa2Cu3O7â^'δ films. Physica C: Superconductivity and Its Applications, 1998, 296, 179-187.	1.2	19
204	The transition from 2D-nucleation to spiral growth in pulsed laser deposited YBa2Cu3O7â^1̂ films. Physica C: Superconductivity and Its Applications, 1998, 305, 1-10.	1.2	27
205	Mechanism of incongruent ablation of SrTiO3. Journal of Applied Physics, 1998, 83, 3386-3389.	2.5	42
206	Crossover between fractal and nonfractal flux penetration in high-temperature superconducting thin films. Physical Review B, 1998, 58, 12467-12477.	3.2	28
207	The relation between the defect structure, the surface roughness and the growth conditions of YBa2Cu3O7â^δ films. Journal of Alloys and Compounds, 1997, 251, 27-30.	5.5	14
208	Twin-free YBa2Cu3O7â^'î´ films on (001) NdGaO3 showing isotropic electrical behaviour. Journal of Alloys and Compounds, 1997, 251, 114-117.	5.5	9
209	The ab-anisotrophy of twinfree YBa2Cu3O7-δ films above and below Tc. Physica C: Superconductivity and Its Applications, 1997, 282-287, 665-666.	1.2	5
210	Magnetic and transport properties of sputtered La0.67Ca0.33MnO3 thin films. Journal of Magnetism and Magnetic Materials, 1997, 165, 380-382.	2.3	16
211	Influence of film growth conditions on the transport properties of YBa2Cu3O7â [~] î [~] step-edge junctions. Applied Superconductivity, 1997, 5, 249-254.	0.5	2
212	Spiral growth in pulsed laser deposited YBa2Cu3O7-δ films. Physica C: Superconductivity and Its Applications, 1997, 282-287, 559-560.	1.2	3
213	Relation between micro-structure and transport properties of epitaxial YBa2Cu3O7â^î^thin films. Physica C: Superconductivity and Its Applications, 1997, 282-287, 2303-2304.	1.2	7
214	Synthesis of yttriumtrihydride films for ex-situ measurements. Journal of Alloys and Compounds, 1996, 239, 158-171.	5.5	113
215	Critical currents and micro-structure in YBa2Cu3O7â~ʾĨ´ thin films. European Physical Journal D, 1996, 46, 1307-1308.	0.4	0
216	Growth and etching phenomena observed by STM/AFM on pulsed-laser deposited YBa2Cu3O7â^'δ films. Physica C: Superconductivity and Its Applications, 1996, 261, 1-11.	1.2	44

#	Article	IF	CITATIONS
217	Stoichiometric transfer of complex oxides by pulsed laser deposition. Applied Surface Science, 1996, 96-98, 679-684.	6.1	24
218	Influence of micro-structure in the low temperature critical currents of YBa2Cu3O7?? thin films. Journal of Low Temperature Physics, 1996, 105, 1017-1022.	1.4	8
219	Stoichiometric transfer of complex oxides by pulsed laser deposition. , 1996, , 679-684.		0
220	Non-Stoichiometric Transfer of Complex Oxides by Pulsed Laser Deposition at Low Fluences. Materials Research Society Symposia Proceedings, 1995, 397, 175.	0.1	3
221	The laser ablation threshold of YBa2Cu3O6+x as revealed by using projection optics. Applied Surface Science, 1995, 86, 13-17.	6.1	17
222	Critical current, magnetization relaxation and activation energies for YBa2Cu3O7 and YBa2Cu4O8 films. Physica C: Superconductivity and Its Applications, 1995, 241, 353-374.	1.2	102
223	NonlinearU(j) dependence determined directly from low-electric-fieldE-jscurves inYBa2Cu3O7â^îthin films. Physical Review B, 1995, 52, 4583-4587.	3.2	21
224	Critical current, magnetization relaxation and activation energies for YBa2Cu3O7 and YBa2Cu4O8 films. Physica C: Superconductivity and Its Applications, 1994, 235-240, 2865-2866.	1.2	2
225	Angular scaling of critical current measurements on laser-ablated YBa2Cu3O7â^î^ thin films. Physica C: Superconductivity and Its Applications, 1994, 235-240, 3053-3054.	1.2	12
226	RBS-PIXE analysis on μm scale on thin film high-Tc superconductors. Nuclear Instruments & Methods in Physics Research B, 1994, 89, 204-207.	1.4	14
227	Laser ablation threshold of YBa2Cu3O6+x. Applied Physics Letters, 1994, 65, 1581-1583.	3.3	72
228	Evidence for mean free path fluctuation induced pinning inYBa2Cu3O7andYBa2Cu4O8films. Physical Review Letters, 1994, 72, 1910-1913.	7.8	301
229	Thermally activated flux motion and quantum creep in YBa2Cu3O7 and Y2Ba4Cu8O16 films. Journal of Alloys and Compounds, 1993, 195, 427-430.	5.5	11
230	Morphology of modulated crystals and quasicrystals. Journal Physics D: Applied Physics, 1991, 24, 186-198.	2.8	12
231	Resistive states in thin films of Y2Ba4Cu8O16â^Î^. Physica C: Superconductivity and Its Applications, 1990, 167, 348-358.	1.2	27
232	Flux creep and critical currents in epitaxial high Tc films. Cryogenics, 1990, 30, 563-568.	1.7	77
233	Buffer layers for superconducting Yî—,Baî—,Cuî—,O thin films on silicon and SiO2. Materials Science and Engineering B: Solid-State Materials for Advanced Technology, 1990, 7, 135-147.	3.5	15
234	Low temperature fluxline relaxation effects in YBa2Cu3O7â^î^thin films. Vacuum, 1990, 41, 862-863.	3.5	0

#	Article	IF	CITATIONS
235	Thermally activated flux motion in high-T c superconductors. Physica C: Superconductivity and Its Applications, 1989, 162-164, 1191-1192.	1.2	11
236	Penetration depth in YBaCuO films. Physica C: Superconductivity and Its Applications, 1989, 162-164, 1563-1564.	1.2	4
237	The morphology of calaverite (AuTe2) from data of 1931. Solution of an old problem of rational indices. Acta Crystallographica Section A: Foundations and Advances, 1989, 45, 115-123.	0.3	36
238	Critical current density and pinning energy of an epitaxial YBa2Cu3O7-δ-film. Physica C: Superconductivity and Its Applications, 1989, 159, 854-862.	1.2	30
239	Field dependence of resistance transitions in thin films of YBA 2 CU 3 O 7 and YBA 2 CU 4 O 8. Physica C: Superconductivity and Its Applications, 1989, 162-164, 1169-1170.	1.2	3
240	Magnetic flux relaxation of epitaxial YBa 2 Cu 3 O 7-δ films at low temperatures Physica C: Superconductivity and Its Applications, 1989, 162-164, 663-664.	1.2	18
241	On the fabrication of flat post-annealed YBa 2 Cu 3 O 7-†films. Physica C: Superconductivity and Its Applications, 1989, 162-164, 705-706.	1.2	2
242	Critical currents and magnetic relaxation of epitaxial YBa2Cu3O7 â^' δ films. Journal of the Less Common Metals, 1989, 151, 39-48.	0.8	37
243	High critical currents and flux creep effects in superconducting YBa2Cu3O7 â~ gd films e-gun deposited using a BaF2 source. Journal of the Less Common Metals, 1989, 151, 325-331.	0.8	20
244	Electron tunnelling and critical current behaviour of patterned Y1Ba2Cu3O7 â^' δ films. Journal of the Less Common Metals, 1989, 151, 435-441.	0.8	1
245	CRITICAL CURRENTS AND MAGNETIC RELAXATION OF EPITAXIAL YBa2Cu3O7–δ FILMS. , 1989, , 39-48.		1
246	ELECTRON TUNNELLING AND CRITICAL CURRENT BEHAVIOUR OF PATTERNED Y1Ba2Cu3O7–δFILMS. , 1989, , 435-441.		0
247	Transmission electron microscopy of thin YBa2Cu3O7â°'x films on (001) SrTiO3 prepared by DC triode sputtering. Journal of Crystal Growth, 1988, 91, 355-362.	1.5	16
248	Flux-creep and critical currents in various YBaCuO-samples. Physica C: Superconductivity and Its Applications, 1988, 153-155, 322-323.	1.2	21
249	Preparation, patterning, and properties of thin YBa2Cu3O7â~î´films. Applied Physics Letters, 1988, 52, 1904-1906.	3.3	46
250	Triode-Sputtered High- <i>T</i> _c Superconducting Thin Films. Europhysics Letters, 1988, 5, 455-460.	2.0	21
251	A synchrotron radiation study of modulated [(CH3)4N]2ZnCl4 crystals. Journal of Applied Crystallography, 1987, 20, 512-516.	4.5	14
252	Crystal form and surface morphology of modulated β-K2SO4-type structures. Acta Crystallographica Section B: Structural Science, 1987, 43, 64-71.	1.8	9

#	Article	IF	CITATIONS
253	The mechanism of tapering on KDP-type crystals. Journal of Crystal Growth, 1986, 74, 118-128.	1.5	52
254	The growth spiral morphology on {100} KDP related to impurity effects and step kinetics. Journal of Crystal Growth, 1986, 76, 243-250.	1.5	65
255	Crystal form and surface morphology of modulated structures. Journal of Crystal Growth, 1986, 79, 811-816.	1.5	3
256	A superspace approach to the structure and morphology of tetramethylammonium tetrachlorozincate, 2C4H12N+.ZnCl4 2â^'. Acta Crystallographica Section B: Structural Science, 1986, 42, 69-77.	1.8	27
257	Incommensurate Morphology of Calaverite (AuTe2) Crystals. Physical Review Letters, 1985, 55, 2301-2304.	7.8	52
258	In SituObservation of a Roughening Transition of the (1012Â ⁻) Satellite Crystal Surface of Modulated ((CH3)N4)Zn2Cl4. Physical Review Letters, 1985, 55, 2806-2809.	7.8	20
259	A "rough heart―model for "edge―dislocations which act as persistent growth sources. Journal of Crystal Growth, 1984, 67, 400-403.	1.5	20
260	In situ observation of surface phenomena on {100} and {101} potassium dihydrogen phosphate crystals. Journal of Crystal Growth, 1984, 69, 306-316.	1.5	40
261	Observation of Bands of Faces on IncommensurateRb2ZnBr4Single Crystals. Physical Review Letters, 1983, 50, 849-852.	7.8	18
262	Morphological determination of modulated-cell parameters of Rb ₂ ZnBr ₄ . Zeitschrift Für Kristallographie, 1983, 165, 247-254.	1.1	16
263	On the formation of etch grooves around stress fields due to inhomogeneous impurity distribution in KH2PO4 single crystals. Journal of Crystal Growth, 1981, 51, 607-623.	1.5	42